Assessing Seal Performance and Parameter Sensitivity with a Full-Shaft Model

MARK REEVES, D.G. FRYAR, and W.H. STATHAM
Duke Engineering & Services, 9111 Research Blvd., Austin TX 78758

and

M.K. KNOWLES
Sandia National Laboratories, WIPP Regulatory Compliance
115 N. Main, Carlsbad NM 88220

INTRODUCTION

The Waste Isolation Pilot Plant (WIPP), is a planned geologic repository for permanent disposal of transuranic waste generated by U.S. government defense programs. Located near Carlsbad in southeastern New Mexico, the facility's disposal regions are mined from the bedded salt of the Salado Formation at a depth of approximately 652 m. Four shafts service the operational needs of the facility for air intake, exhaust, waste handling, and salt handling. These shafts range in diameter from 3.5 to 6.1 m and extend from the ground surface to the repository. During repository closure, following an operational life of approximately 50 years, these shafts will be sealed in accordance with an acceptable design. Under contract to the U.S. Department of Energy (DOE), the Repository Isolation Systems Department (RISD) of Sandia National Laboratories has developed a design for the WIPP shaft sealing system. This design has been reviewed by the U.S. Environmental Protection Agency (EPA) as part of the 1996 WIPP Compliance Certification Application (CCA).

An effective shaft sealing system for the WIPP will limit liquid and gas flows, and permanently prevent the migration of radiological or other hazardous constituents through the sealed shafts from repository to accessible environment. Because of these performance objectives, a significant effort has been directed toward evaluation of the seal design. Whereas RISD (1996) provides a comprehensive discussion, this paper focuses on only one aspect of the evaluation effort, namely a full-shaft, fluid-flow model.

DESCRIPTION OF THE PHYSICAL SYSTEM

Two principal elements comprise the WIPP shaft seal system, specifically the seal, which includes individual sealing components, and the surrounding host rock geology, which includes both disturbed and undisturbed rock. As illustrated in Figure 1a, the shafts pass through three different formations as they extend from ground surface to the repository horizon, and the proposed seal design comprises thirteen different seal components. These components fill the entire shaft volume with a variety of low-permeability materials, including compacted bentonite clay, compacted crushed Salado salt, and asphalt. Concrete, used in strategic locations, provides an immediate low-permeability, structural support for sealing and construction needs.

Beginning 15 to 30 m below surface (Figure 1a), the Dewey Lake Redbeds consist of alternating layers of sandstone and siltstone. This formation is not known to have laterally extensive saturated zones. For this reason, Dewey-Lake seal components are meant primarily to eliminate surface access to the shafts and to limit surface-water infiltration. They are not considered by the fluid-flow analyses. Lying immediately below the Dewey Lake Redbeds and composed primarily of anhydrite and dolomite layers, the Rustler Formation contains the only laterally extensive, water-bearing units at the site.

Below the Rustler Formation, the Salado Formation represents a Permian-age evaporite sequence composed of bedded halite, polyhalite, anhydrite, and mudstone lithologic units Several of the thicker layers of Salado anhydrites and polyhalites are designated as "marker beds." Although all Salado units have very low permeabilities, some of the marker beds are more transmissive than the halitic sequences. Furthermore, within the WIPP shafts, several brine-seepage intervals have been noted. These intervals were assigned permeabilities which are an order-of-magnitude higher than values

assigned to marker beds of similar composition. For all the various materials comprising this system, RISD (1996), Appendix C, reports values and sources for the hydraulic parameters, including relative-permeability and capillary-pressure curves.

MODEL CONCEPTUALIZATION

Model Grid. Considering the Air Intake Shaft (AIS) to be representative of the other three shafts, the axisymmetric grid chosen for the analysis extends from the shaft station monolith at a depth of 652 m up to the top of the Rustler Formation at a depth of 162 m. Horizontally, the grid extends radially outward from the center of the shaft to the shaft wall at a radius of 3.09 m and to an outer radius of 30.9 m. Row thicknesses and column widths are chosen judiciously in order to represent both stratigraphy and seal components. These include a concrete liner in the upper portion of the shaft terminated by a "key" at the Rustler-Salado Transition and a disturbed rock zone (DRZ) surrounding both as it extends the full length of the shaft. The grid contains 19 columns and 99 layers.

Boundary Conditions. Invoking a code revision to TOUGH28W, the numerical solution at the outer boundary of the gridded region was coupled to the analytic solution for an infinite aquifer using the approximation of Carter and Tracy (1960). In effect, then, a constant-pressure boundary was applied at infinite radius. Generally, no-flow conditions were applied at the upper and lower boundaries. However, after repository closure, corrosive and/or biochemical reactions in the waste forms may generate hydrogen gas which, over time, could elevate pressures at the bottom of the shaft. After consulting earlier studies (DOE, 1995 and RISD, 1996, Appendix C), we assumed that the boundary pressure increases linearly from zero to 7 MPa in 100 years and remains constant thereafter.

Initial Conditions. Various authors (Mercer, 1983 and Beauheim, 1987) have recognized that *in-situ* pressures within the Rustler and Salado Formations are not in hydrostatic equilibrium. Furthermore, records indicate that, for the latter formation, only two pressure measurements exist, one at the Rustler-Salado Transition and the other at Marker Bed MB139, just below the repository horizon. Considering the likelihood that some portion of the lithostatic load is transferred to Salado fluids, the study developed three initial-pressure distributions, *e.g.,* compare the base-case run with Runs 2 and 8 (Table 1).

DRZ Healing. As a result of stress-induced fracturing, DRZs form around excavations, yielding increased values of permeability and porosity in affected regions. Since the existence of a shaft DRZ raises the possibility of a permeable vertical conduit, it was considered carefully in the design and evaluation efforts. For the Salado subsystem, the seal design (Figure 1a) includes three concrete/asphalt waterstop components which both provide backpressure for DRZ healing and intersect the DRZ with waterstops, low-permeability components containing asphalt.

For the brittle material of the Rustler Formation, no DRZ healing is expected. However, for the Salado Formation, mechanical calculations (RISD, 1996, Appendix D) show that, following closure, the radial extent of the DRZ decreases as a function of time, depth, seal material, and rock type. Using a code revision to TOUGH28W, the present study includes this effect as a monotonically decreasing DRZ permeability. Mechanical calculations (RISD, 1996, Appendix D) also indicate that, for anhydrite and dolomite units of sufficient thickness, stress-induced fracturing does not occur, thus making the DRZ discontinuous. However, after considering construction effects such as blasting damage or the known natural fracturing of dolomites at the WIPP site, the present study assumed a continuous DRZ for the base-case and used a case involving a discontinuous DRZ (Run 7, Table 1) to test for sensitivity.

Fractured/Unfractured DRZ. For the Room Q studies, Munson *et al.* (1996) use the SPECTROM-32 code (Callahan, 1994 and Callahan *et al.* ,1989) to characterize the DRZ. The results divide volumetric strain into elastic and inelastic components giving each as a function of radius and time. If, like Freeze *et al.* (1997), we identify inelastic strain with fracture porosity, then the work of Munson *et al.* (1996) shows that by approximately eight years, the fracture porosity ϕ_f reaches asymptotic values lying within the range $10^{-4} \le \phi_f \le 10^{-3}$, approximately, depending on radial distance from the room face. For the present study, the base case assumes that the DRZ may be satisfactorily approximated as an unfractured medium with altered properties relative to undisturbed rock. To investigate possible effects due to a fracturing, Runs 1, 2, and 3 (Table 1) characterize the DRZ by an effective-continuum permeability model (Pruess *et al.*, 1988) with representative values of fracture porosity.

Salt-Column Consolidation. One of the primary seal components in the Salado Subsystem is composed of crushed salt (see Figure 1a). During emplacement, this material will be dynamically compacted to a density approaching 90 percent of intact salt. Over time, it is assumed that compactional loading due to the creep of intact salt will consolidate the crushed salt and reduce its permeability to a level which is nearly indistinguishable from the host rock.

Two components make up the crushed-salt permeability model, the first of which is density. Since no field analogs exist from which crushed-salt density can be inferred for long times, mechanical analyses were performed to predict density as a function of time, depth, and pore pressure. The second component of the permeability model is a relationship between density and permeability. Here, the effort considered three different experimental studies involving the permeability of consolidated crushed salt (Brodsky, 1994; Hansen and Ahrens, 1996; and Brodsky *et al.,* 1996). Analysis then gave a log-linear relation between permeability and density.

RESULTS

The full-shaft simulations presented here consider two time periods. For the 50-year preclosure period, shaft pressures are fixed at one atmosphere, and host-rock pressures are initialized at *in-situ* levels. For the second, a 200-year postclosure period, shaft-seal pressures are initialized at one atmosphere and allowed to vary, while host-rock pressures are initialized at levels determined by the preclosure simulation. Other simulations consider a 10,000-year postclosure period (RISD, 1966, Appendix C, and Dennis *et al*, 1998).

Verification Results. In an attempt to verify the numerical model, the study reviewed shaft-inflow estimates for the preclosure period (see LaVenue *et al.*, 1990). Prior to lining, estimated inflow rates range from a high of 3,469 m^3/y in 1981 at the Salt Handling Shaft to a minimum of 252 m^3/y in 1987 at the Waste Handling Shaft. After lining, estimated inflow rates range from no observable flow to values as high as those observed prior to lining. Various grouting campaigns have targeted and stopped significant inflows, thus reducing these values. Simulated results give a 50-year annual average of 15.5 m^3/y for the period following lining. Given the level of uncertainty present in the estimated inflow rates and the fact that early-time estimates would be substantially greater than a 50-year annual average, we consider the agreement between estimated and simulated values to be satisfactory.

Base-Case Results. Figure 1b characterizes the liquid resaturation process. The figure shows that, although substantial levels of liquid resaturation have occurred within the seal by 40 years, a major gas pocket remains at Layers 22 - 32 and a minor such pocket remains at Layers 43 - 45. This is significant since both are located in the salt column, and the lowest permeability levels are correlated with gas pockets. For the Salado Formation, one may also note the role of the combined units (marker beds) in resaturating the Salado portion of the seal (Layers 1 - 80).

Sensitivity Results. Table 1 defines 13 runs, the results of which may be compared with those of the base case. These runs probe the seal, DRZ, and host rock seeking significant sensitivities. Consistent with objectives of the study, two performance measures are used to characterize hydrologic performance. Cumulative flows through and/or around the concrete/waterstop components quantify the movement of liquid and gas. Salt-column permeability levels quantify the degree of consolidation of the compacted salt column and its effectiveness in limiting fluid and gas flows.

Generally, one may assume that, after 200 years, backpressures are sufficiently large to prevent further consolidation. Thus, the salt-column permeabilities given in Table 1 represent asymptotic values. Generally, these permeability values are quite low, *i.e.*, approximately one order-of-magnitude greater than that assumed for intact salt (10^{-21} m^2). However, Runs 6, 10, and 11 evidence a strong sensitivity to marker-bed permeability. Here, an order-of-magnitude increase in permeability (Run 11) increases salt-column permeability by four orders of magnitude to 4.35×10^{-16} m^2.

CONCLUSIONS

Except for marker-bed permeability, salt-column permeability evidenced an impressive list of insensitivities. Tests to date indicate that uncertainties in Salado *in situ* pressures, in characterizing the DRZ as fractured or porous, and uncertainties in the fracturing of the thicker anhydrite and dolomite

DRZs do not significantly affect performance. Similarly, altering the seal design by removing the three asphalt waterstops, by removing the middle concrete/waterstop component, or by replacing the asphalt column (10^{-20} m^2) with a more permeable clay column (10^{-15} m^2) do not affect performance. Finally, neither setting all seal-component permeabilities (except that for crushed salt) to their maximum values (RISD, 1996, Appendix C) nor reducing all clay permeabilities from their base-case value of 5×10^{-19} m^2 to 10^{-14} m^2 impact salt-column performance.

For cumulative flows through and/or around concrete/waterstop components, the study calculated 84 different values. Consequently, the results are more difficult to summarize than those obtained for the first performance measure. Suffice it to say that, at the lower concrete/waterstop component, the maximum downwardly directed flow of brine occurred for Run 11. Here, an order-of-magnitude increase in marker-bed permeabilities and a consequent increase in salt-column permeability by four orders of magnitude yielded approximately 2000 kg (1.7 m^3) of brine during the 200-year period following repository closure. This flow exceeds that of the base case by less than a factor of two. Also, at the upper concrete/waterstop component, the maximum upwardly directed flow of gas occurred for Run 5. Here, increasing all seal permeabilities (except that of the salt column) to the maximum permitted by their respective uncertainty ranges yielded approximately 5.6 kg (62 standard m^3) of hydrogen over the 200-year period following repository closure. This flow, though small, exceeds that of the base case by two orders of magnitude.

The results of this study thus reveal a robust seal design which can withstand variations in properties of the seal components and most uncertainties present in both disturbed and undisturbed rock zones. The results also suggest that uncertainties present in marker-bed permeabilities can impact salt-column performance.

REFERENCES

Beauheim, R.L. 1987. *Interpretations of Single-Well Hydraulic Tests Conducted at and Near the Waste Isolation Pilot Plant (WIPP) 1983-1987.* SAND87-0039. Albuquerque, NM: Sandia National Laboratories.

Brodsky, N.S. 1994. *Hydrostatic and Shear Consolidation Tests with Permeability Measurements on Waste Isolation Pilot Plant Crushed Salt.* SAND93-7058. Albuquerque, NM: Sandia National Laboratories.

Brodsky, N.S., F.D. Hansen, and T.W. Pfeifle. 1996. "Properties of Dynamically Compacted Crushed Salt, *Montreal, Quebec, June 17-18, 1996."* SAND96-0838C. Albuquerque, NM: Sandia National Laboratories. (Copy on file at the Technical Library, Sandia National Laboratories.)

Callahan, G. D. 1994. *SPECTROM-32: A Finite Element Thermomechanical Stress Analysis Program Version 4.06,* RSI-0531, prepared by RE/SPEC Inc., Rapid City, SD, for Sandia National Laboratories, Albuquerque, NM.

Callahan, G. D., A. F. Fossum, and D. K. Svalstad. 1989. *Documentation of SPECTROM-32: A Finite Element Thermomechanical Stress Analysis Program*, DOE/CH/10378-2, prepared by RE/SPEC Inc., Rapid City, SD, for the U.S. Department of Energy, Chicago Operations Office, Argonne, IL, Vol. I and II.

Carter, R.D. and C.W. Tracy. 1960. "An Improved Method for Calculating Water Influx", *Transactions of the Society of Petroleum Engineers, American Institute of Mining Engineers*, pp. 219, 415-417.

Dennis, A.W., J.D. Tillerson, J.D. Schreiber, P. Vaughn, and J.F. Bean. 1988. "Waste Isolation Pilot Plant (WIPP) Shaft Seal System Performance Sensitivity and Design Impact." To be presented at the International High-Level Radioactive Waste Management Conference, Las Vegas, NV. May 11-14, 1988.

DOE (U.S. Department of Energy). 1995. *Waste Isolation Pilot Plant Sealing System Design Report.* DOE/WIPP-95-3117. Carlsbad, NM: U.S. Department of Energy, Waste Isolation Pilot Plant.

Freeze, G.A., T.L. Christian-Frear, and S.W. Webb. 1997. *Modeling Brine Inflow to Room Q: A Numerical Investigation of Flow Mechanisms*. SAND96-0561. Albuquerque, NM: Sandia National Laboratories.

Hansen, F.D., and E.H. Ahrens. 1996. "Large-Scale Dynamic Compaction of Natural Salt," *4th International Conference on the Mechanical Behavior of Salt, Montreal, Quebec, June 17-18, 1996"* SAND96-0792C. Albuquerque, NM: Sandia National Laboratories.

LaVenue, A.M, T.L. Cauffman, and J.F. Pickens. 1990. *Ground-Water Flow Modeling of the Culebra Dolomite. Volume I: Model Calibration.* SAND89-7068/1. Albuquerque, NM: Sandia National Laboratories.

Mercer, J.W. 1983. *Geohydrology of the Proposed Waste Isolation Pilot Plant Site, Los Medanos Area, Southeastern New Mexico.* Water-Resources Investigations Report 83-4016. Albuquerque, NM: U.S. Geological Survey.

Munson, D. E., A.L. Jensen, S.W. Webb, and K.L. DeVries. 1996. "Brine Release Based on Structural Calculations of Damage Around an Excavation at the Waste Isolation Pilot Plant (WIPP)", *2nd North American Rock Mechanics Conference , Montreal, Canada, June 17-19, 1996.* SAND95-1704C. Albuquerque, NM: Sandia National Laboratories.

Pruess, K., J.S.Y. Wang, and Y.W. Tsang. 1988. *Effective Continuum Approximation for Modeling Fluid and Heat Flow in Fractured Porous Tuff.* SAND86-7000. Albuquerque, NM: Sandia National Laboratories.

Pruess, K. 1991. *TOUGH2 - A General-Purpose Numerical Simulator for Multiphase Fluid and Heat Flow.* LBL-29400. Berkeley, CA: Earth Sciences Division, Lawrence Berkeley Laboratory.

RISD (Repository Isolation Systems Department). 1996. *Waste Isolation Pilot Plant Shaft Sealing System Compliance Submittal Design Report. Volume 1&2:* SAND96-1326/1&2. Albuquerque, NM: Sandia National Laboratories.

Table 1. Sensitivity Simulations for the Shaft Seal System

Simulation	DRZ		Initial Condition	Parameter Varied	Salt Column Permeability at 200 Years
	Cont.	Fract.			
Base	Yes	No	Fractional lithostatic	---	2.39×10^{-20} m^2
Run 1	Yes	Yes	Fractional lithostatic	Fracture porosity = 10^{-3}	1.43×10^{-20} m^2
Run 2	Yes	Yes	Interpolated	Fracture porosity = 10^{-3}	1.41×10^{-20} m^2
Run 3	Yes	Yes	Fractional lithostatic	Fracture porosity = 10^{-4}	1.77×10^{-20} m^2
Run 4	Yes	No	Fractional lithostatic	Clay k = 10^{-14} m^2	2.40×10^{-20} m^2
Run 5	Yes	No	Fractional lithostatic	All seal k to maximum	2.52×10^{-20} m^2
Run 6	Yes	No	Fractional lithostatic	MB k increased x 2	1.46×10^{-19} m^2
Run 7	No	No	Hydrostatic	Discontinuous DRZ	2.18×10^{-20} m^2
Run 8	Yes	No	Hydrostatic	Hydrostatic initial cond.	2.51×10^{-20} m^2
Run 9	Yes	No	Fractional lithostatic	No water stops	2.50×10^{-20} m^2
Run 10	Yes	No	Fractional lithostatic	MB k increased x 5	1.20×10^{-16} m^2
Run 11	Yes	No	Fractional lithostatic	MB k increased x 10	4.35×10^{-16} m^2
Run 12	Yes	No	Fractional lithostatic	Removed Middle Concrete	2.22×10^{-20} m^2
Run 13	Yes	No	Fractional lithostatic	Asphalt Col Replaced w/ Clay (k = 10^{-15} m^2)	2.39×10^{-20} m^2

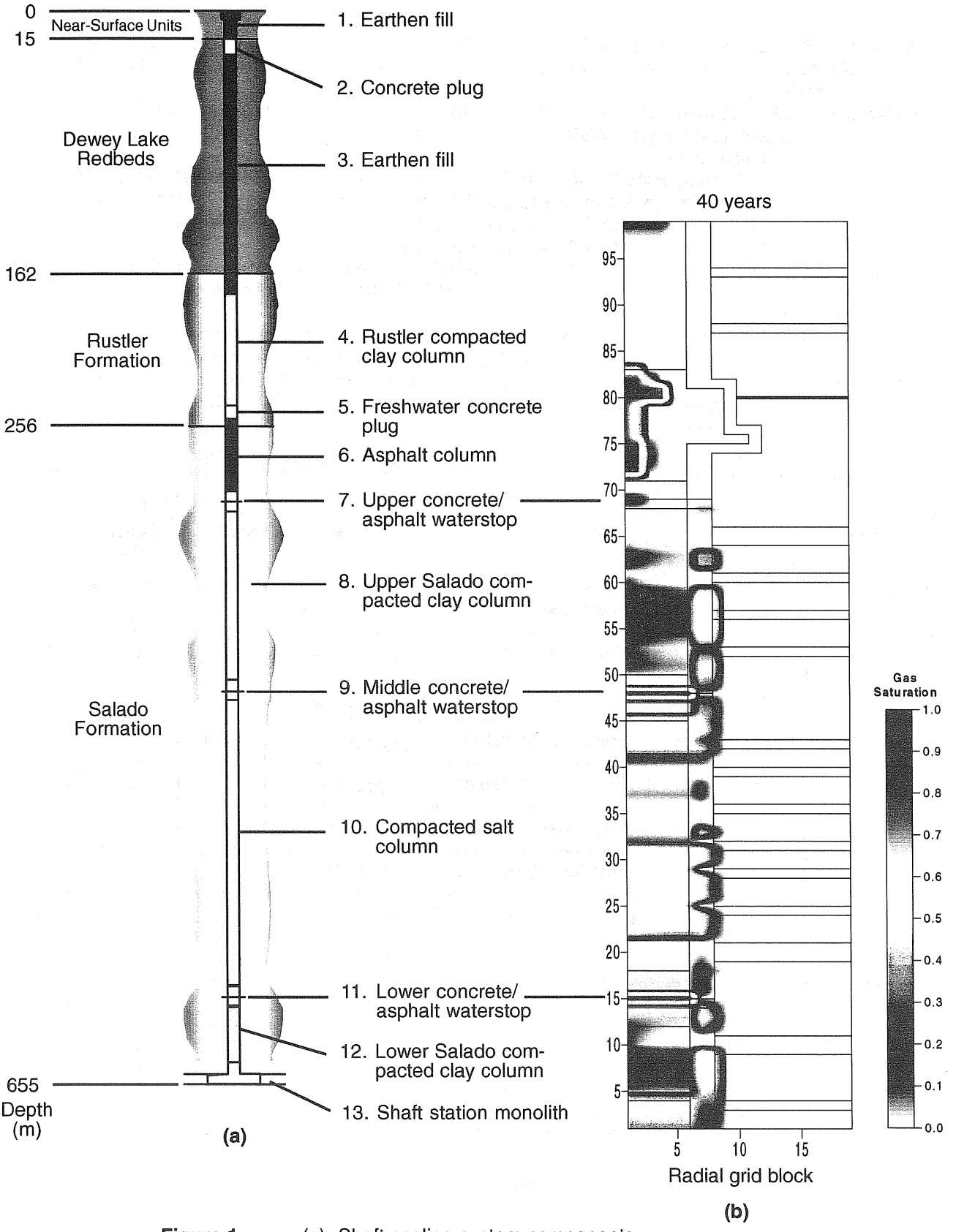

Figure 1: (a) Shaft sealing system components
(b) Base-case gas distribution, 40 years after closure